Ocean Engineering 96 (2015) 205–214

Contents lists available at ScienceDirect

Ocean Engineering

journal homepage: www.elsevier.com/locate/oceaneng

An axisymmetric underwater vehicle-free surface interaction: A numerical study

Ali Nematollahi [a], Abdolrahman Dadvand [b,*], Mazyar Dawoodian [b]

[a] Department of Mechanical Engineering, University of Manitoba, Winnipeg, Canada MB R3T 5V6
[b] Department of Mechanical Engineering, Urmia University of Technology, Urmia 419-57155, Iran

ARTICLE INFO

Article history:
Received 30 March 2014
Accepted 20 December 2014

Keywords:
Viscous resistance
Wave-making resistance
Underwater vehicle
Free surface
Numerical simulation

ABSTRACT

Underwater vehicles (UWVs) have been widely used in oceanographic applications. Investigation of their interaction with free surface when they are moving near the free surface is of great importance. In the present work, the hydrodynamic characteristics of a standard UWV (Afterbody-1) moving in water and its interaction with free surface are studied numerically using CFD software ANSYS^{TM} CFX. The total drag coefficient including the viscous and wave-making resistances acting over the UWV for its operating speeds ranging from $0.4\,m/s$ ($Re = 1.05 \times 10^5$) to $1.4\,m/s$ ($Re = 3.67 \times 10^5$) at different depths of submergence ranging from 0.75 to 4.0, is obtained. Also the wake formed behind the UWV is characterized to better understand the hydrodynamic behavior of the UWV motion in water at different submergence depths and vehicle speeds. The results were compared with available measured data and good agreements were observed. It was found that, for all submergence depths as the Reynolds number was increased the drag coefficient was decreased. Besides, for a fixed Reynolds number as the submergence depth was decreased the drag coefficient was increased. Finally, for small submergence depths the effect of UWV motion on the free surface became more appreciable if the Reynolds number was increased.

1. Introduction

Autonomous Underwater Vehicles (AUVs) or simply Underwater Vehicles (UWVs) have increasingly found many ocean applications such as ocean surveillance and measurements, exploration and exploitation of seafloor minerals, environmental monitoring and protection and deep-sea exploration of hydrocarbons (Jagadeesh and Murali, 2010; Saout and Ananthakrishnan, 2011). AUVs can be subdivided into three broad types based on operating regime: bottom layer, interior and surface layer (Curtin et al., 2005). Bottom layer AUVs would operate as a transport, tanker and relative navigation reference. Interior class AUVs would serve as a mobilesensor and are capable of navigating and communicating throughout the water column. Surface layer AUVs would act as communication links between the acoustic transmissions of the interior and bottom layer AUVs and the above surface radio transmissions. The interaction between the free-surface and an AUV could be significant in littoral applications and when the AUV traverses near the free surface. In open ocean applications, an AUV would experience the free-surface effects periodically, particularly when it has to surface to get GPS fixes for navigation (Saout and Ananthakrishnan, 2011). This emphasizes the need for better understanding of the hydrodynamic forces acting on the underwater bodies under various conditions. Such understanding would help designing more efficient powering systems for the AUV.

There have been a number of experimental investigations on axisymmetric underwater bodies (Gertler, 1950; Granville, 1953; Nakayama and Patel, 1974; Patel and Lee, 1977; Huang et al., 1978; Roddy, 1990; Dash et al., 1996; Hackett, 2000; Jagadeesh et al., 2009; Jagadeesh and Murali, 2010). Most of these studies have been conducted in a wind tunnel. Zedan and Dalton (1979) made a critical comparison between the drag characteristics based on volume, surface area and frontal area for different axisymmetric bodies. Sayer (1996) conducted experimental tests to measure the drag and added mass coefficients on a remotely operated vehicle and a solid box for various submergence depths in a towing tank.

Although experimental tests are very useful for determining resistance and power requirements of UWVs, computational fluid dynamics (CFD) can be used efficiently for the same purpose. The CFD procedure is shown to be capable of reproducing the experimental investigations quite well. Several researchers (Patel and Chen, 1986; Choi and Ching, 1991; Sung et al., 1993, 1995; Sarkar et al., 1997a, b; Ananthakrishnan and Zhang, 1998; Mulvany et al., 2004; Jagadeesh and Murali, 2006) investigated various issues related to the application of CFD to underwater hydrodynamics. The influences of turbulence models, grid generation, boundary resolution techniques and

* Corresponding author. Tel.: +98 4413980264; fax: +98 4413554184.
E-mail address: a.dadvand@mee.uut.ac.ir (A. Dadvand).

http://dx.doi.org/10.1016/j.oceaneng.2014.12.028
0029-8018/

boundary conditions on CFD solutions, etc. were investigated over axisymmetric bodies. The studies suggest that the force coefficients vary significantly as a function of depth of submergence.

The total resistance (drag) against the motion of a body in water comprises two components: viscous and pressure resistances, which are known respectively as viscous and wave-making resistances for vehicles traveling on or near the free surface. Although there are several investigations on the hydrodynamics of two- and three-dimensional bodies submerged in water and on their interaction with the free surface, most of these studies considered the hydrofoil geometry and merely the wave-making resistance and were generally based on the potential theory (Sahin et al., 1997; Ahmed and Soares, 2009; Zhang et al., 2009; Chen and Zhu, 2010; Saout and Ananthakrishnan, 2011). It may be noted that potential theory does not consider the effects of viscosity or separation of the flow around the body although empirical knowledge can be included to account for these effects.

In the present work, the hydrodynamic characteristics of a standard UWV (Afterbody-1) motion in water and its interaction with free surface are studied numerically. The total drag coefficient acting over the UWV for its operating speeds ranging from 0.4 m/s ($Re = 1.05 \times 10^5$) to 1.4 m/s ($Re = 3.67 \times 10^5$) at different depths of submergence H ranging from 0.75 to 4.0, is obtained. In addition, the wake behind the UWV is characterized to better understand the hydrodynamic behavior of the UWV motion in water at different submergence depths and vehicle speeds. It is worth mentioning that, in CFD simulation of flow over UWVs, proper selection of turbulence model is a key issue that can directly affect the simulation accuracy and efficiency. The simulation of underwater hydrodynamics continues to be based on the solution of the Reynolds-averaged Navier Stokes (RANS) equations. The RANS based simulations are much more dependent on the selection of suitable turbulence model. In the current investigation, numerical studies are conducted using standard $k-\varepsilon$ turbulence model in the commercial flow solver CFX (CFX, 2012). The computed drag force coefficients are compared with the measured data of Jagadeesh et al. (2009), and Jagadeesh and Murali (2010).

2. Governing equations and numerical implementation

2.1. Problem description

The UWV (Afterbody-1) configuration and dimensions, which are chosen based on the work by Jagadeesh and Murali (2010), are shown in Fig. 1. The UWV is submerged at a distance h below the initially undisturbed free surface of water. The maximum diameter of the UWV is D. Due to the presence of free surface, the acceleration due to gravity g exerts an influence on the UWV motion and must be considered. The important physical parameters characterizing the flow state are the Reynolds number $Re = \rho U \nabla^{1/3}/\mu$, the Froude number Fr, and the initial UWV-free surface distance, $H = h/D$, where ρ is density of water (1000 kg/m^3), U is the inlet velocity, and ∇ is volume of the body (0.018 m^3), and μ is the viscosity of water (0.001 kg/m s).

2.2. Governing equations

The steady, incompressible, viscous and turbulent flow field around the UWV can be simulated by solving the RANS equations where the Reynolds stress $\overline{u_i u_j}$ is replaced with the standard $k-\varepsilon$ turbulence model. The governing equations of the flow field and mathematical expression of the standard $k-\varepsilon$ turbulence model are described below (Liu and Guo, 2013):

(i) The RANS equations

$$\text{Continuity}: \quad \frac{\partial U_j}{\partial x_j} = 0 \tag{1}$$

$$\text{Momentum}: \quad \frac{\partial U_i}{\partial t} + \left(U_j \frac{\partial U_i}{\partial x_j} + \frac{\partial \overline{u_i u_j}}{\partial x_j} \right) = -\frac{\partial p}{\partial x_i} + \frac{1}{Re} \nabla^2 U_i \tag{2}$$

(ii) The $k-\varepsilon$ equations

$$\frac{\partial k}{\partial t} + \left(U_j - \frac{1}{\sigma_k} \frac{\partial \nu_t}{\partial x_j} \right) \frac{\partial k}{\partial x_j} = \frac{1}{R_k} \nabla^2 k - G + \varepsilon \tag{3}$$

$$\frac{\partial \varepsilon}{\partial t} + \left(U_j - \frac{1}{\sigma_\varepsilon} \frac{\partial \nu_t}{\partial x_j} \right) \frac{\partial \varepsilon}{\partial x_j} = \frac{1}{R_\varepsilon} \nabla^2 \varepsilon + \frac{\varepsilon}{k} (C_{\varepsilon 1} G - C_{\varepsilon 2} \varepsilon) \tag{4}$$

where U_i denotes the mean velocity components, p is the pressure, and G is the turbulence production term, which can be expressed as:

$$G = \nu_t \left(\frac{\partial U_i}{\partial x_j} + \frac{\partial U_j}{\partial x_i} \right)^2 \tag{5}$$

where $\nu_t = C_\mu k^2/\varepsilon$ denotes eddy viscosity. The relationship between Reynolds stress $\overline{u_i u_j}$, turbulence kinetic energy k and turbulence dissipation ε and eddy viscosity is written as:

$$-\overline{u_i u_j} = \nu_t \left(\frac{\partial U_i}{\partial x_j} + \frac{\partial U_j}{\partial x_i} \right) - \frac{2}{3} \delta_{ij} k \tag{6}$$

The values of constant coefficients C_μ, $C_{\varepsilon 1}$, $C_{\varepsilon 2}$, σ_k and σ_ε are set equal to 0.09, 1.44, 1.92, 1.0 and 1.3, respectively. The effective viscosities R_k and R_ε are taken as $1/R_k = (1/Re) + (\nu_t/\sigma_k)$ and $1/R_\varepsilon = (1/Re) + (\nu_t/\sigma_\varepsilon)$, respectively.

The main computational difficulty in the present work is related to the deformable free-surface. There are various ways to treat this situation numerically. A potential constraint in this case is that the surface may form breaking waves at high Froude numbers, which means that computational methods that track the surface directly as a computational boundary may fail or have difficulties. In order to tackle the problem, the interface capturing volume-of-fluid (VOF) method was used. Here, both the liquid phase (water) and the much

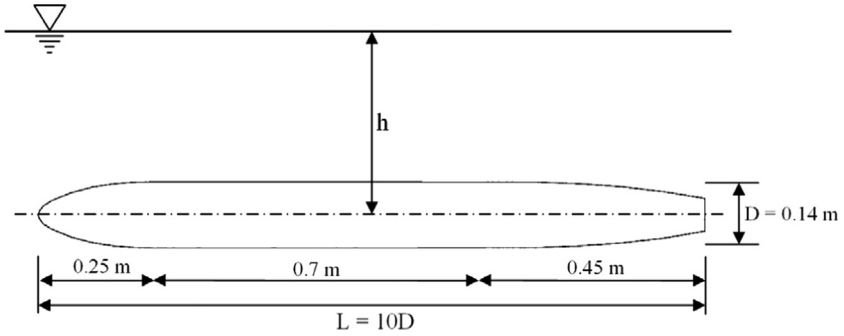

Fig. 1. UWV configuration and dimensions.